RESEARCH ARTICLE

Journal of Cellular Physiology WILEY

Zika virus alters osteogenic lineage progression of human mesenchymal stromal cells

Noreen Mumtaz[1] | Amel Dudakovic[2] | Asha Nair[2] | Marijke Koedam[3] | Johannes P. T. M. van Leeuwen[3] | Marion P. G. Koopmans[1] | Barry Rockx[1] | Andre J. van Wijnen[4] | Bram C. J. van der Eerden[3]

[1]Department of Viroscience, Erasmus MC, Erasmus University Medical Centre, Rotterdam, The Netherlands

[2]Departments of Orthopedic Surgery and Biochemistry and Molecular Biology, Mayo Clinic, Rochester, Minnesota, USA

[3]Department of Internal Medicine, Erasmus MC, Erasmus University Medical Centre, Rotterdam, The Netherlands

[4]Department of Biochemistry, University of Vermont College of Medicine, Burlington, Vermont, USA

Correspondence
Bram C. J. van der Eerden, Department of Internal Medicine, Laboratory for Calcium and Bone Metabolism, Erasmus MC, Erasmus University Medical Center, room Ee585b, Dr Molewaterplein 40, Rotterdam 3015 GD, The Netherlands.
Email: b.vandereerden@erasmusmc.nl

Barry Rockx, Department of Viroscience, Erasmus MC, Erasmus University Medical Center, Dr Molewaterplein 40, Rotterdam 3015 GD, The Netherlands.
Email: b.rockx@erasmusmc.nl

Abstract

Arboviruses target bone forming osteoblasts and perturb bone remodeling via paracrine factors. We previously reported that Zika virus (ZIKV) infection of early-stage human mesenchymal stromal cells (MSCs) inhibited the osteogenic lineage commitment of MSCs. To understand the physiological interplay between bone development and ZIKV pathogenesis, we employed a primary in vitro model to examine the biological responses of MSCs to ZIKV infection at different stages of osteogenesis. Precommitted MSCs were infected at the late stage of osteogenic stimulation (Day 7) with ZIKV (multiplicity of infection of 5). We observe that MSCs infected at the late stage of differentiation are highly susceptible to ZIKV infection similar to previous observations with early stage infected MSCs (Day 0). However, in contrast to ZIKV infection at the early stage of differentiation, infection at a later stage significantly elevates the key osteogenic markers and calcium content. Comparative RNA sequencing (RNA-seq) of early and late stage infected MSCs reveals that ZIKV infection alters the mRNA transcriptome during osteogenic induction of MSCs (1251 genes). ZIKV infection provokes a robust antiviral response at both stages of osteogenic differentiation as reflected by the upregulation of interferon responsive genes ($n > 140$). ZIKV infection enhances the expression of immune-related genes in early stage MSCs while increasing cell cycle genes in late stage MSCs. Remarkably, ZIKA infection in early stage MSCs also activates lipid metabolism-related pathways. In conclusion, ZIKV infection has differentiation stage-dependent effects on MSCs and this mechanistic understanding may permit the development of new therapeutic or preventative measures for bone-related effects of ZIKV infection.

KEYWORDS
bone formation, mesenchymal stromal cells, osteoblast, Zika virus

1 | INTRODUCTION

Zika virus (ZIKV) was first isolated in 1947 from a rhesus monkey in Uganda (Brasil et al., 2016). From the 1960s to the 1980s, ZIKV cases of human infections were rarely found across Asia and Africa (Bordi et al., 2017). ZIKV has become more of a global threat because of its emergence and spread around the globe over the last decade, especially after the first major outbreak of ZIKV occurred in 2007 in the Yap Islands of Micronesia (Lanciotti et al., 2008), followed by another large outbreak in 2013 in French Polynesia (Sikka et al., 2016). More recently, the ZIKV spread into and beyond Brazil in 2015–2016, with the further geographic expansion of ZIKV in the United States (Marcondes & Ximenes, 2016; White et al., 2016).

The clinical presentation of acute symptomatic ZIKV infections in adults is generally mild with symptoms similar to that of other arboviruses, such as Dengue virus (DENV), Chikungunya virus (CHIKV), and Ross River virus (RRV) (Alshammari et al., 2018; Haddow et al., 2012), and includes osteoarticular complications like articular joint pain (arthralgia) (Brasil et al., 2016; Colombo et al., 2017; Wimalasiri-Yapa et al., 2020). The bone-related complaints may present in patients because ZIKV and other arboviruses can infect the cell types, such as osteoblasts and osteoclasts, which play an essential role in bone remodeling (Borgherini et al., 2008; W. Chen et al., 2014; Huang et al., 2016; Mumtaz et al., 2018). Intriguingly, microcephaly observed in ZIKV-infected pregnant women has been linked to infection of cranial neural crest cells (CNCCs), which give rise to cranial bones and influence the developing brain (Bayless et al., 2016; Del Campo et al., 2017; Chung et al., 2009). Furthermore, observations with a fetus from a ZIKV-infected pregnant woman revealed that ZIKV exhibits tropism to mesenchymal stromal cells (MSCs), which represent fibroblastic precursors of bone-forming osteoblasts (van der Eijk et al., 2016). This osteo-tropism of ZIKV suggests a direct possible link between ZIKV infection and bone-related clinical outcomes.

In our previously published study, we reported that ZIKV infected osteoprogenitor cells and affected the differentiation and mineralization (Mumtaz et al., 2018). Previously, we infected the osteoblast precursors at early stage of differentiation, and did not determine if the effect of infection is stage dependent. Differentiation of MSCs into osteoblasts is a multistep process and several key regulators of differentiation and maturation tightly regulate distinct stages with characteristic biomarkers (Stephens et al., 2011). Therefore, in this follow-up study, we determined the susceptibility of late stage MSCs, to ZIKV infection and monitored the replication kinetics and effects of ZIKV infection on osteogenic differentiation. Since we found phenotypic differences between early and late stage MSC, we performed comparative transcriptome profiling of ZIKV infected cells at different stages of osteogenic differentiation (early and late stage) to gain initial insights into regulatory pathways linked to osteoarticular complications. Our results identified key pathways associated with ZIKV infection that depend on the stage of osteogenic differentiation in MSCs.

2 | MATERIALS AND METHODS

2.1 | Cell culture

Human bone marrow-derived MSCs from healthy male donors were purchased from Lonza (PT-2501). MSCs were confirmed ≥90% positive for CD105, CD166, CD29, & CD44 and ≤10% positive for CD14, CD34, & CD45. These MSCs were subjected to osteogenic differentiation over a period of 2–3 weeks as described previously (Both et al., 2017). Briefly, differentiation into calcium depositing osteoblasts was initiated on Day 3 post-seeding (Day 0—osteogenic stimulation; Figure 1) and alpha minimum essential medium containing 50 mM ascorbic acid was supplemented with 100 mM dexamethasone (dex) and 10 mM β-glycerophosphate (osteogenic medium) (Bruedigam et al., 2011). Vero
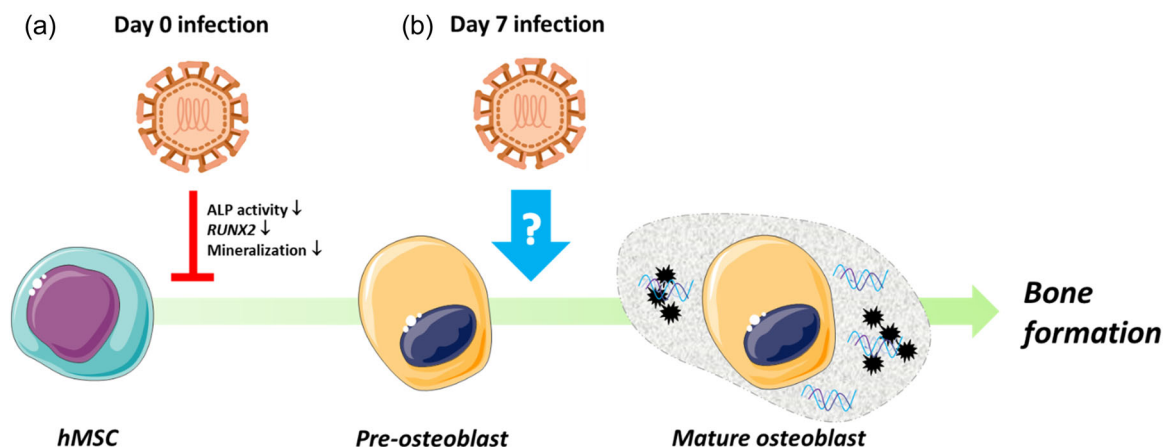

FIGURE 1 Schematic overview of the ZIKV infection regimen relative to osteogenic differentiation of human mesenchymal stromal cells (hMSCs). Bone marrow-derived hMSCs undergo osteogenic differentiation through preosteoblasts into mature, mineralizing osteoblasts. (a) Our previous data demonstrated that ZIKV infection of MSCs during early differentiation stages (Day 0) reduced their differentiation and maturation potential compared to mock-infected controls. (b) Our present studies aim to assess the susceptibility of MSCs to ZIKV infection during later stages of osteogenic differentiation (Day 7 poststimulation). ZIKV, Zika virus.

cells (African green monkey kidney epithelial cells, ATCC CCL-81) were maintained to perform ZIKV replication kinetics. Cells were cultured in Dulbecco's modified Eagle's medium (Lonza) supplemented with 10% heat-inactivated fetal bovine serum (Greiner Bio-One), 2 mM L-glutamine, 1% sodium bicarbonate, 1% HEPES, 100 U/ml penicillin, and 100 μg/ml streptomycin (all from Lonza) at 37°C and 5% CO_2 in a humidified atmosphere.

2.2 | Virus

ZIKV strain Suriname ZIKVNL00013 (ZIKVAS-Sur16; EVAg no. 011V-01621) was grown in Vero cells and passage number 3 was used for the current study. Virus titers in the supernatants were determined as described previously (Mumtaz et al., 2018).

2.3 | Replication kinetics of ZIKV in late infected MSCs

ZIKV replication in late infected MSCs was determined as described previously (Mumtaz et al., 2018). Briefly, MSCs were subjected to osteogenic induction for 7 days and then infected at a multiplicity of infection (MOI) of 5 with ZIKV for 1 h at 37°C in 5% CO_2. After incubation, the supernatant was removed and cells were cultured in an osteogenic medium. Cells were refreshed twice a week for approximately 2 weeks. Mock-infected controls were cultured in parallel. To determine the titers produced by ZIKV infection, cell supernatants were collected at different time points postinfection. The supernatant was stored at −80°C for titration. Experiments were performed in triplicate.

2.4 | Immunofluorescence assay (IFA)

Infected cells from the replication growth kinetics assay were fixed with 4% PFA at Day 4 postinfection, permeabilized with 70% ethanol, and stained for ZIKV virus with mouse monoclonal antibody anti-flavivirus group antigen (MAB 10216), clone D1-4G2-4-15 (Millipore), using an IFA as described previously (Mumtaz et al., 2018). For alkaline phosphatase (ALP) and ZIKV costaining, late stage infected MSCs were fixed and stained at Days 4 and 7 postinfection (Days 11 and 14 post-osteogenic stimulation). Infected and uninfected controls were stained for ZIKV and ALP with humanized IgG1 pan-flavivirus antibody 4G2 (hu4G2; Native Antigen Company) and mouse anti-human ALP (Abcam) followed by staining with the goat anti-human IgG conjugated with Alexa Fluor 488 (Life Technologies) and Alexa Fluor 555-conjugated donkey anti-mouse IgG (Life Technologies), respectively.

2.5 | ALP, mineralization, and protein assays

ALP and calcium measurements were performed as described previously (Bruedigam et al., 2011; Granchi et al., 2010). Briefly,

ALP activity was determined by measuring its conversion of para-nitro phenyl phosphate (pNPP) (Sigma) to paranitrophenol for 10 min at 37°C and measured at 405 nm, using a Victor2 plate reader. ALP results were adjusted for protein content of the cell lysates as described before (Mumtaz et al., 2018). Calcium measurements were performed after overnight incubation of cell lysates with 0.24 M HCl at 4°C. Calcium content was determined calorimetrically using a calcium assay reagent prepared by combining 1 M ethanolamine buffer (pH 10.6) with 0.35 mM O-cresolphthalein complex one in a ratio of 1:1. All measurements were done at 595 nm using a Victor2 plate reader.

2.6 | RNA preparation

To perform host transcriptomic analysis, MSCs (Donor# 1) were subjected to osteogenic stimulation and were infected at different stages of differentiation; at Day 0 (early) and Day 7 (late) post-osteogenic stimulation with ZIKV at a MOI of 5 for 1 h at 37°C in 5% CO_2. For both ZIKV-infected treatment groups and the corresponding mock-infected control, total RNA was extracted on Day 15 post-initial osteogenic induction of MSCs using TRIzol reagent (Thermo Fisher Scientific). RNA was purified with the miRNAeasy mini kit (Qiagen). The quantity and integrity of RNA were assessed by ultraviolet absorbance using a NanoDrop device (Thermo Fisher Scientific) and RNA integrity number (RIN score) (Agilent Technologies). High throughput RNA sequencing (RNA-seq) was carried out using cDNA samples that were indexed using TruSeq Kits. The library size distribution was examined using an Agilent Bioanalyzer DNA 1000 chip and Qubit fluorometry (Invitrogen) followed by the generation of paired-end sequencing reads on an Illumina HiSeq. 2000 sequencer as described previously (Dudakovic et al., 2014; Lewallen et al., 2021).

2.7 | Bioinformatics analysis of RNA-seq data

Raw RNA-seq reads were aligned and normalized by the MAP-RSEq (v.1.2.1) workflow, which incorporates Top Hat and HTSEq, to generate expression values expressed as Fragments Per Kilobase of transcript per Million mapped reads (FPKM) as described in detail previously (Dudakovic et al., 2014; Kalari et al., 2014; Lewallen et al., 2021). Identification of differentially expressed genes (DEGs) was performed using DEseq (Love et al., 2014) with adjusted p values using the Benjamini−Hochberg method. DEGs were filtered for minimal expression (FKPM >0.3), biologically relevant fold changes (|Log2 FC| >1), and statistical significance ($p < 0.05$).

2.8 | Pathway and functional enrichment analysis

Functional enrichment and pathway analyses were carried out using the web-based tools DAVID v 6.8 (Dennis et al., 2003) and Ingenuity pathway analysis software (IPA, http://www.ingenuity.com/index.

html). Gene ontology (GO) terms and pathways were considered enriched when their Benjamini−Hochberg-corrected enrichment p-value was below 0.05.

2.9 | Quantification of mRNA expression

For gene expression validation by qPCR, RNA from ZIKV infected or mock infected MSCs were used for cDNA synthesis and PCR reactions as described previously (Bruedigam et al., 2011). Oligonucleotide primer pairs were designed to be either on exon boundaries or spanning at least one intron. Data are presented as relative mRNA levels calculated by the formula: $2^{-\Delta\left(C_t \text{ of a gene of interest} - C_t \text{ of housekeeping gene}\right)}$. All primer sequences used are summarized in Table 1.

2.10 | Statistical analysis

Statistical analyses of quantitative values obtained by biochemical analysis including ALP activity, calcium deposition, and qPCR validation of mRNAs, were performed using Graph Pad Prism 9 software. All results are expressed as means with a standard error of the mean. Mann−Whitney U test was used for the comparison between two groups (infected vs. uninfected). $p \leq 0.05$ was considered significant.

3 | RESULTS

3.1 | ZIKV replicates in MSCs to high titers

We have previously shown that MSCs at early stages of osteogenic differentiation are susceptible to infection with ZIKV, resulting in persistent infection in the absence of cytopathic effect (Mumtaz et al., 2018) (Figure 1). To determine whether MSCs in later stages of osteogenic differentiation are also susceptible to infection with ZIKV, we performed ZIKV infections at an MOI of 5 in osteogenically differentiated MSC cultures after 1 week of incubation in osteogenic media. These late stage infected MSCs (Day 7) were highly susceptible to ZIKV infection without any evidence of cytopathic effects. ZIKV infected osteogenically induced MSCs produced high infectious titers of up to $10^{6.5}$ TCID$_{50}$/ml within 4 days postinfection. Virus growth kinetics showed that these differentiating MSCs were persistently infected with ZIKV and shedding of infectious virions was observed over the entire 2-week period postinfection (Figure 2a). ZIKV infection of MSCs was confirmed by IFA on Day 4 postinfection (Figure 2b,c).

TABLE 1 Primer sequences of the analyzed genes

Gene	Forward primer (5′-3′)	Reverse primer (5′-3′)
ASPM	TTTACAGATCAGAAGCAGTGTTATC	TCTCCTCCACATAGCCTGAA
B2M	GATGAGTATGCCTGCCGTGT	CTGCTTACATGTCTCGATCCCA
CD36	GACCCTGAGGCCAGGATCTA	GGATGCAGCTGCCACAG
DPP4	GAGATGTTCCGGTCCTGGTC	TCCAGGACTCTCAGCCCTTT
GAPDH	CCGCATCTTCTTTTGCGTCG	CCCAATACGACCAAATCCGTTG
IFI27	CGGCCATTGCCAATGG	AGAGTCCAGTTGCTCCCAGTGA
IFI44	GGCAGAAGGAGCAGGACTGT	GGTTTACGGGAATTAAACTGATATCTGT
IFIT1	TCCTTGGGTTCGTCTACAAATTG	TCAAAGTCAGCAGCCAGTCTCA
IFNB	CTAGCACTGGCTGGAATGAGACTA	CCAGGACTGTCTTCAGATGGTTT
IRF9	GCCCTACAAGGTGTATCAGTTGCT	TCGCTTTGATGGTACTTTCTGAGT
ISG20	GATGCCGGCTTGGAGTTAGA	GACCCTCAGAGATGCTGCC
OAS1	TGTGTGTCCAAGGTGGTAAAGG	CAACCAGGTCAGCGTCAGATC
PRLR	ACTTGCCTCTTTCTCCAG	TCCCTCAAGAATACTAAGCAG
RUNX2	GATTACAGACCCCAGGCAGG	GGCTCAGGTAGGAGGGGTAA
STAT1	TCTGTGTCTGAAGTTCACCCT	ACAGAGCCCACTATCCGAGA
TACSTD	TCACGCTTCCTGATTCCTCG	GACCCTGAGGCCAGGATCTA

Abbreviations: ASPM, assembly factor for spindle microtubules; B2M, beta-2-microglobulin; DPP4, dipeptidyl peptidase-4; GAPDH, glyceraldehyde 3-phosphate dehydrogenase; IFI27, interferon alpha inducible protein 27; IFI44, interferon induced protein 44; IFIT1, interferon induced protein with tetratricopeptide repeats 1; IFNB, interferon β; IRF9 interferon regulatory factor 9; ISG20, interferon stimulatory gene 20; OAS1, 2′-5′-oligoadenylate synthetase 1; PRLR, prolactin receptor; RUNX2, RUNX family transcription factor 2; STAT1, signal transducer and activator of transcription 1; TACSTD, tumor associated calcium signal transducer 2.
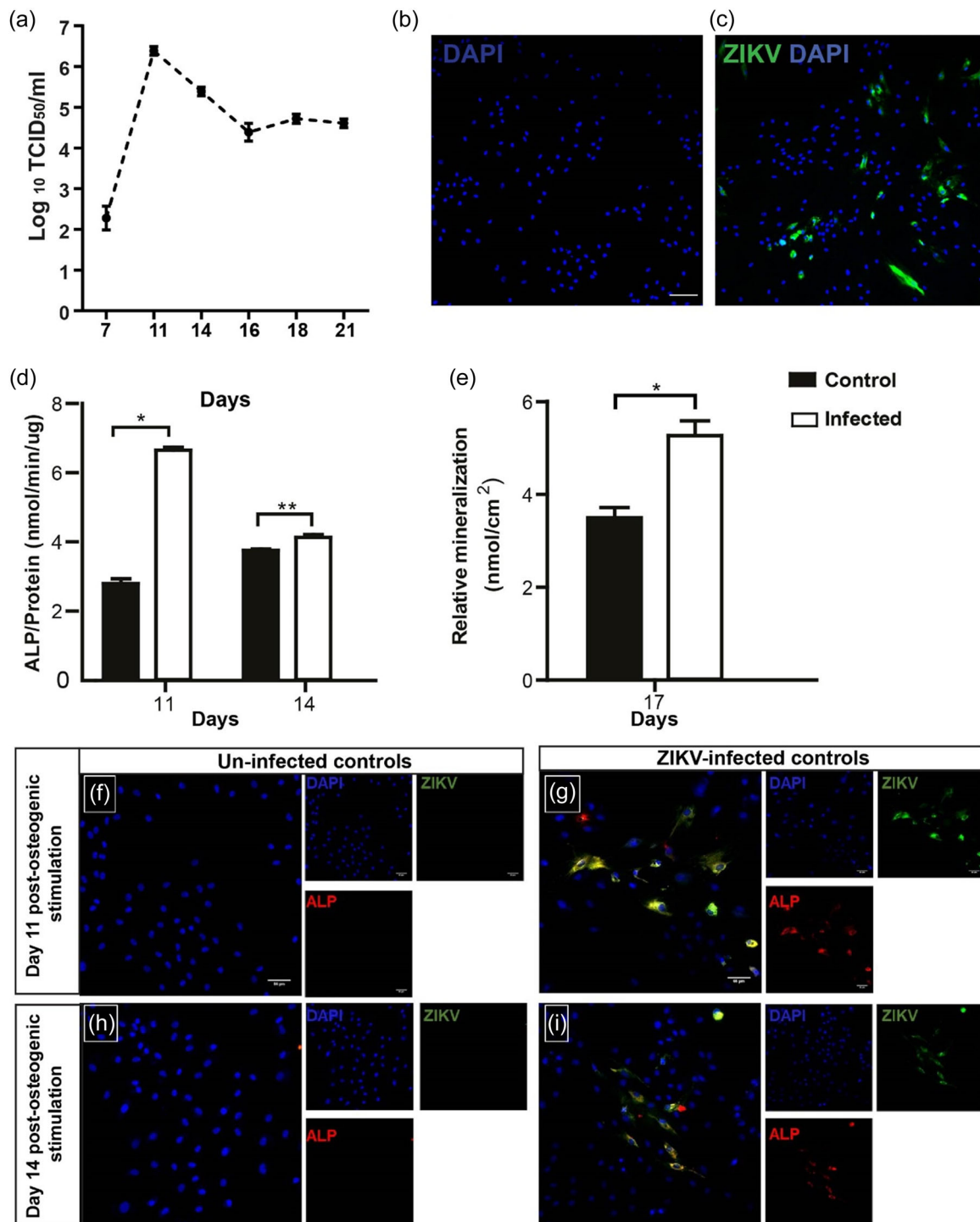
FIGURE 2 Replication and osteogenic effects of ZIKV in late stage infected MSCs. (a) Line plot showing the growth curve kinetics (log10 TCID50/ml) of ZIKV infection during MSCs differentiation over a period of 14 days. (b–c) Immunofluorescent images of uninfected mock (b) and ZIKV-infected cells (c) stained for ZIKV antigen (green) and nuclei (blue) at Day 4 postinfection (magnification X100). (d, e) Bar plots showing the effect of infection on osteoblast differentiation as assessed by ALP (d) and mineralization measured by calcium contents (e), respectively. (f–i) Immunofluorescent images of uninfected mock (f–h) and ZIKV-infected cells (g–i) stained for ZIKV antigen (green), ALP (red), and nuclei (blue) at Days 4 and 7 postinfection (magnification X100). All biochemistry assays were performed in triplicates. Each experiment has n = 3–4 biological replicates depending on the assay. Representative results from an independent experiment are shown in (d, e) from Donor #1. Results are compared between ZIKV infected (white bars) and uninfected controls (black bars) and ALP levels are normalized against the total protein. Error bars represent the SEM. *p < 0.05. ALP, alkaline phosphatase; MSCs, mesenchymal stromal cells; SEM, standard error of the mean; ZIKV, Zika virus.

3.2 | ZIKV infection of maturing osteoblasts induces osteogenesis

To determine the effect of ZIKV infection in late stages of osteogenic differentiation of MSCs, ALP activity, and calcium deposition were quantified at different time points (Days 11, 14, and 17) post-osteogenic stimulation. For late stages of infection, we did not measure RUNX2 expression because we and others have previously shown that RUNX2 is only elevated during the early stages of MSCs differentiation where the commitment of osteoblast precursors to osteogenic lineage is determined (Mumtaz et al., 2018). In late staged MSCs infected with ZIKV, we only quantified ALP activity and mineralization as markers of osteoblast differentiation. ALP activity was significantly increased on Days 11 and 14 post-osteogenic stimulation compared to uninfected controls (Figure 2d). ZIKV infection also increased calcium deposition in ZIKV-infected MSCs compared to uninfected controls at 17 days post-osteogenic stimulation (Figure 2e). To determine if ZIKV infection directly affected the expression of ALP in infected late staged MSCs, or whether this was a by-stander effect, we performed IFA for ALP and viral antigen at Days 11 and 14 post-osteogenic stimulation. We selected these time points based on our functional data for ALP activity. By IFA, we detected an elevated ALP expression almost exclusively in ZIKV infected cells, but not in uninfected cells, for both time points (Figure 2f–i). These data suggest that the increased ALP activity is due to an increase in ALP expression in ZIKV infected cells.

We observed consistent phenotypic effects, regarding ZIKV replication and increased osteogenesis, in another tested donor (#2) (Supporting Information: Figure 1–3). Thus, while our previously published study showed reduced differentiation in ZIKV infected MSCs at early stages of osteogenic lineage commitment (Mumtaz et al., 2018), the current study revealed that ZIKV infection at later stages of osteogenic induction increases their differentiation compared to mock-infected controls (Figure 2d,e). These diverging results suggest that the effect of ZIKV infection depends on the stage of differentiation.

3.3 | Differential regulation of gene expression in ZIKV-infected MSCs at early versus later stages of osteogenic differentiation

To identify the molecular pathways associated with this differentiation dependent outcome of ZIKV infection, we performed next generation sequencing-based RNA expression analyses for ZIKV infected MSCs and mock-infected controls at the stage of robust calcium deposition (Day 15). The primary comparison is between early versus later infected cells, and as an expression baseline, we used mock-infected MSCs. Our mock control set is pooled data from early ($n = 2$) and late ($n = 2$) uninfected cells, and both hierarchical clustering and heat-map analysis indicate that these four samples group together. Therefore, mock controls are grouped for the subsequent analysis. To identify the spatial distribution between two groups: ZIKV infected (early vs. later stage MSCs), and mock-infected MSCs, we performed principal component analysis (PCA). The PCA showed that all three conditions were separated into three different clusters based on three principal components explaining, respectively, 40.3%, 27.7%, and 19.1% of the total variance (total >87%) within the RNA-seq data (Figure 3a). PCA analysis also showed a larger variance between the replicates of the late stage MSC group compared to the early stage MSC and mock-infected groups. The heat-map of DEGs showed that all three replicates of ZIKV infected early stage MSCs showed similar gene expression profiles, with two clusters of up- and downregulated genes compared to mock-infected controls (Figure 3b). Gene expression profiles for replicates of ZIKV infected later stage MSCs also appeared similar except that one cluster of genes exhibits intragroup variability between the replicates, corroborating observations with the PCA plot (Figure 3a,b). Compared with mock-infected controls, ZIKV infected later stage MSCs showed two large clusters where genes are differentially expressed. Interestingly, in one of the two clusters, genes were upregulated in ZIKV infected at later stage MSCs compared with mock infected controls, and ZIKV infected early stage MSCs. Additionally, DEGs with a high fold change (>Log 2-fold) differences between ZIKV infected MSCs compared with mock-infected controls are visualized in volcano plots (Figure 3c,d), respectively. There are predominantly upregulated genes (~251) in ZIKV infected early stage MSCs compared with mock-infected controls (Figure 3c). This plethora of upregulated genes may represent an initial cell response to viral infection. In contrast to early stage MSCs, the distribution of DEGs is nearly symmetrical for ZIKV infected later stage MSCs (i.e., 588 up- and 444 downregulated genes).

3.4 | Stage-specific functional enrichment in early versus later stage MSCs

Global gene expression analyses showed a higher number of DEGs (≥Log 2-fold) in ZIKV infected later stage MSCs compared to infected early stage MSCs (1034 and 360, respectively) (Figure 4a). The lists of genes for early and late stage infected MSCs (Donor # 1) with fold change differences are provided in Supporting Information:- Tables 1–3. The majority of DEGs are unique to each group of ZIKV infected MSCs. However, 143 DEGs were common between the two treated groups (Figure 4b) of which the majority was regulated in the same direction for both stages. To provide a functional interpretation to the differentially regulated gene sets in the unique and common groups, we performed a GO-based enrichment analysis using a web-based tool (DAVID 6.8). Functional enrichment analysis was performed separately based on the list of DEGs unique to and common between ZIKV infected MSCs (Figure 4c–e). For early stage MSCs, the most significant GO terms are related to extracellular space, antiviral defense and lipid metabolism (Figure 4c). For ZIKV infected later stage MSCs, the most enriched terms are cell cycle, microtubule binding and activity, and DNA synthesis, and repair (Figure 4d). For the gene set overlapping between the two groups of
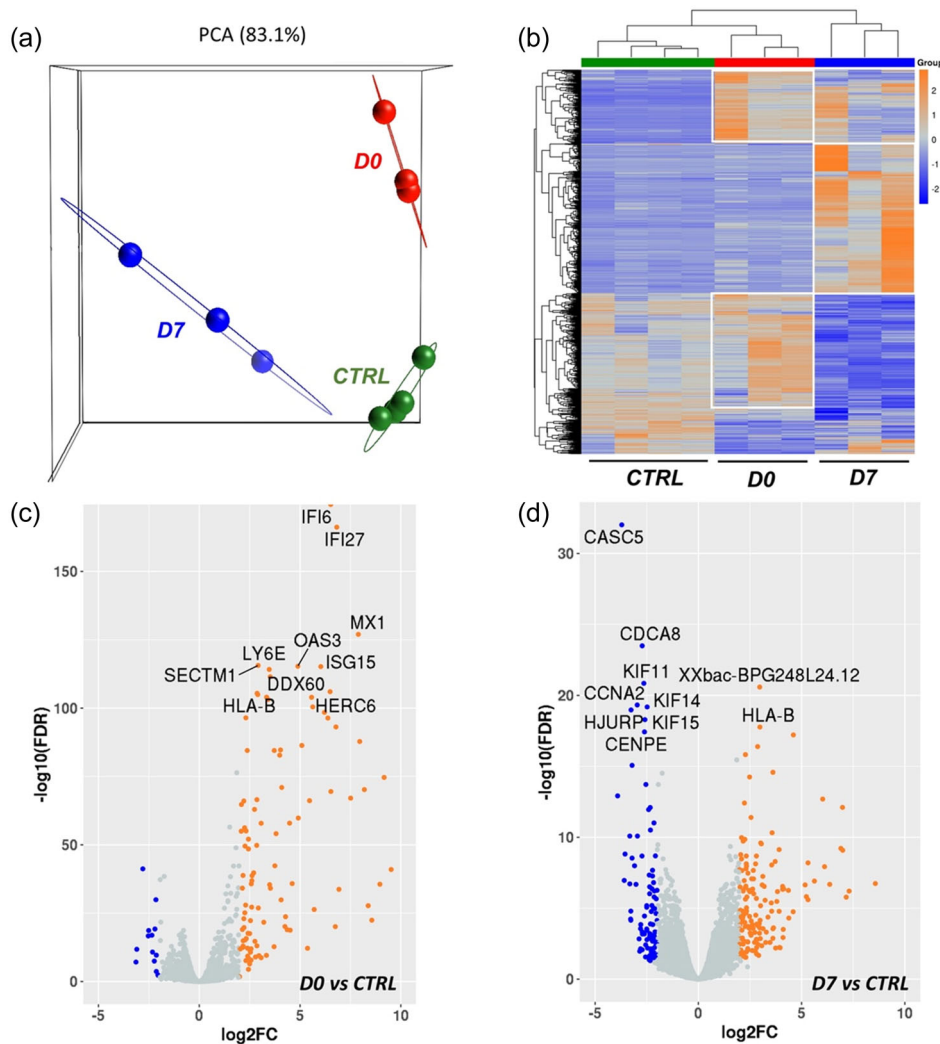
FIGURE 3 RNA sequence analyses of ZIKV-infected and mock-infected late stage MSCs. (a) Principal component analysis (PCA) plot based on ZIKV-infected groups (Day 0 infected: red; Day 7 infected: blue) and mock-infected controls (green). (b) Heat map of differentially expressed genes (DEGs) in ZIKV infected (Day 0: red; Day 7: blue) and mock-infected cells (green). (c−d) Volcano plots highlighting the top significantly regulated genes in Day 0 infected (c) and Day 7 Infected (d) MSCs (upregulated: red; downregulated: green). Visualization of the heat map and volcano plot is performed by RNA-seq. For figures (b−d), a threshold of $\log_2$ FC> 2 with an FDR <0.05 was used to identify the DEGs. Each treated group has n = 3 replicates. MSCs, mesenchymal stromal cells; RNA-seq, RNA sequencing; ZIKV, Zika virus.

ZIKV infected MSCs, we found primarily enrichment of antivirus response-related terms (Figure 4e).

In parallel, we performed IPA based on the same DEGs to determine the canonical pathways. As shown in Figure 5, IPA highlighted functional networks, based on distinct genes (nodes) and their interactions (edges) in canonical pathways that are mentioned in the tables underneath. In the pathway enrichment analysis of ZIKV infected early stage MSCs, we found that most of the upregulated genes were associated with immune responses including granulocyte adhesion and diapedesis, and cholesterol metabolism such as LXR/ RXR activation. The pathway analysis of unique genes for ZIKV infected later stage MSCs showed that DEGs were associated with cell cycle and mitotic division as observed in functional enrichment analysis (Figure 5b). Similar to DAVID6.8 annotation cluster analysis, the overlapping genes between the two groups of ZIKV infected

MSCs revealed immune response-related pathways as major pathways being affected due to ZIKV infection (Figure 5c).

3.5 | Expression of cell surface receptors that accommodate ZIKV entry

We also assessed whether mRNAs for proteins that support infection of ZIKA in MSCs are expressed or not. Arboviruses enter cells via members of the MERTK/AXL/TYRO3 receptor kinase family, as well as CD209 (DC-SIGN) and HAVCR1 (TIM-1) (Perera-Lecoin et al., 2013). Therefore, we extracted the relative read counts for these genes from our RNA-seq data, while calculating the average, standard deviation and coefficient of variation (=STD/average; n = 12). MSCs do not express *MERTK*, *CD209* (DC-SIGN), or *HAVCR1*,
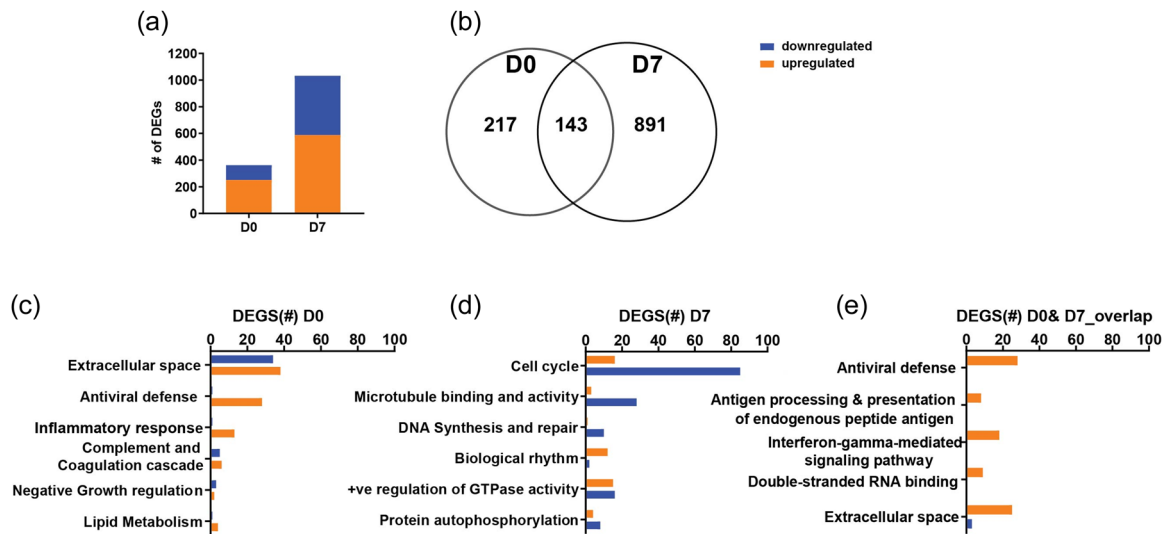
FIGURE 4 Functional enrichment analyses of differentially expressed genes (DEGs) in ZIKV infected early—(D0) and late stage (D7) MSCs. (a) Bar plot with a comparison of up- and downregulated DEGs in Days 0 and 7 infected osteoblasts. (b) Venn diagram with unique and overlapping DEGs for ZIKV infected early and late stage MSCs. (c–d) Functional enrichment analyses for Day 0 infected OBs (c), and Day 7 infected OBs (d) with unique DEGs. (e) Functional enrichment analysis for ZIKV infected early and late stage MSCs with overlapping DEGs. Each treated group has $n = 3$ replicates. MSCs, mesenchymal stromal cells; ZIKV, Zika virus.
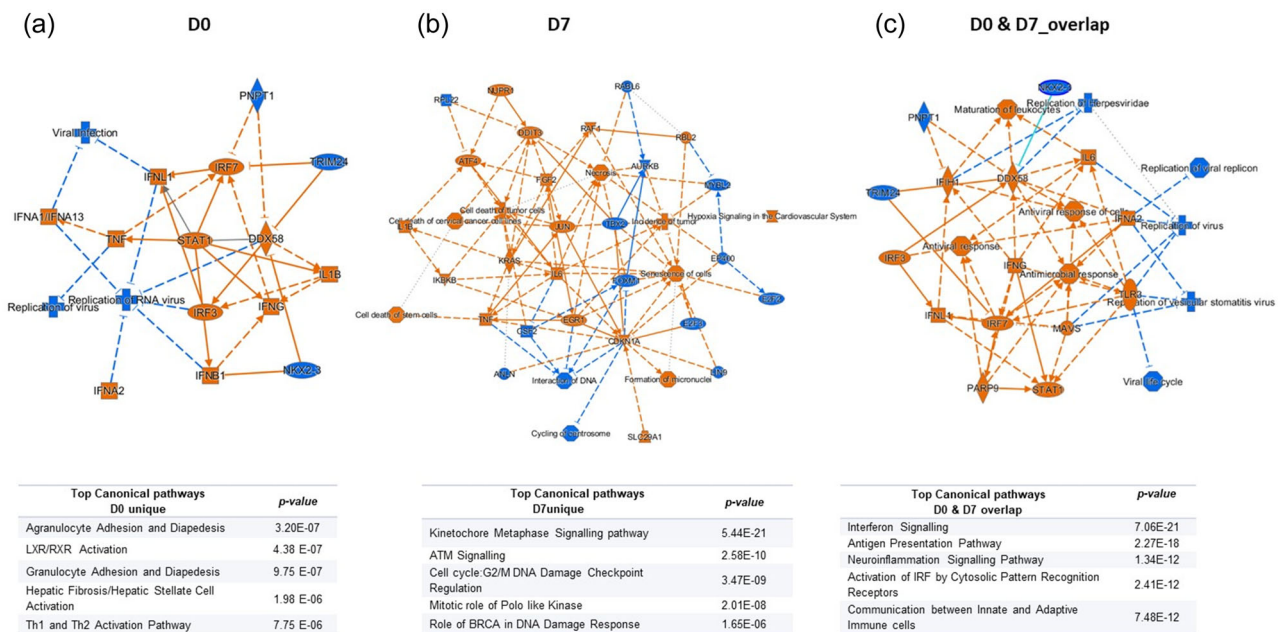

FIGURE 5 Pathway enrichment analyses based on DEGS in ZIKV infected early—(D0) and late stage (D7) MSCs. (a–b) Representations of the network built using unique DEGs in ZIKV infected early (a) and late stage MSCs (b). (c) Network of DEGs based on overlapping genes between ZIKV infected early and late stage MSCs. Ingenuity pathway analysis (IPA) was used to generate the networks overlaid with relative gene expression levels measured in ZIKV infected early and late stage of differentiating MSCs from Donor #1. For network analyses, a threshold of log2 FC >2 with an FDR <0.05 was used to identify differentially expressed genes. Node color represents upregulated (orange) and downregulated (blue) genes. DEGs, differentially expressed genes; MSCs, mesenchymal stromal cells; ZIKV, Zika virus.

nor do they express the mRNA encoding the COVID19 receptor (*ACE2*) as an outgroup comparison. However, these cells express high levels of *AXL* mRNA (FKMP = 76.89 ± 5.72) and low levels of *TYRO3* mRNA (FKPM = 4.71 ± 0.90) across all samples analyzed (*n* = 12). The mRNA levels for AXL and TYRO3 are virtually constant, because their

standard deviations are minimal (with low coefficients of variation of, respectively, 0.07 and 0.19; *n* = 12), regardless of whether MSCs are infected or not. The robust expression of *AXL* mRNA indicates that the encoded protein may represent the primary entry point for ZIKA infection in differentiating MSCs—as was shown for other cell types

(J. Chen et al., 2018; Hamel et al., 2015; Meertens et al., 2017; Nowakowski et al., 2016), with perhaps a secondary role for TYRO3. In addition, the invariability of AXL and TYRO3 expression in both ZIKV-infected and mock-treated MSCs indicates that ZIKV does not directly control mRNA expression of proteins that support its infectious cycle via host cell entry (assuming this indeed is the entry pathway).

3.6 | Quantitative reverse transcription PCR (qRT-PCR) validation of differentially regulated genes in ZIKV infected osteogenically induced MSCs

To validate the gene expression profiles of DEGs identified by RNA-Seq from a single donor, we performed real time qRT-PCR analysis for a select set of genes representative of interferon (IFN), immune-related, or other pathways, from two distinct donors with the same phenotype, including, *CD36, IFIT1, IFI27, IFI44, IFNB, IRF9, OAS1, RUNX2, STAT1, TACSTD* (Figure 6a–j and Supporting Information: Figure 2), and *ASPM, B2M, CD36, DPP4, IFI27, IFI44, IFIT1, IRF9, ISG20, OAS1, PRLR, STAT1* (Figure 7a–l and Supporting Information: Figure 3). The selected genes are differentially regulated between ZIKV infected MSCs and mock infected controls. The qRT-PCR results for selected DEGs identified by RNA-seq analysis showed good agreement with the expression patterns of RNA-seq analysis.

4 | DISCUSSION

Bone-related pathologies are known for several arboviruses, including but not limited to ZIKV, DENV, CHIKV, and RRV (W. Chen et al., 2015; Cui et al., 2018; Sissoko et al., 2009). Other clinically relevant studies have shown that ZIKV exhibits tropism for MSCs which are precursors for bone forming osteoblasts, in the perichondrium of an infected fetus (van der Eijk et al., 2016). In addition, we previously demonstrated that ZIKV infection impaired the function of osteogenically induced MSCs when infected at early stage of differentiation (Mumtaz et al., 2018). Here, we report that osteogenically induced MSCs remain susceptible to ZIKV infection at later stages of osteoblast lineage progression. RNA-seq data indicate that MSCs express very robust levels of AXL mRNA that encodes the potential receptor for arbovirus entry, thus clarifying the tropism for ZIKV. Remarkably, while ZIKV inhibits early stages of osteogenic lineage commitment in MSCs by affecting the levels of RUNX2 (early stage marker) and ALP activity (differentiation marker) (Mumtaz et al., 2018), we find that ZIKV infection accelerates differentiation of later stage committed MSCs, as shown by elevated ALP activity and calcium deposition. These findings regarding the levels of ALP and the subsequent effect on calcium deposition are usually strongly correlated, including in our work (Brum et al., 2015; Eijken et al., 2006). In addition, the increased ALP activity was a direct effect of ZIKV infection-induced ALP expression. Accelerated osteogenesis causes premature fusion of cranial sutures associated
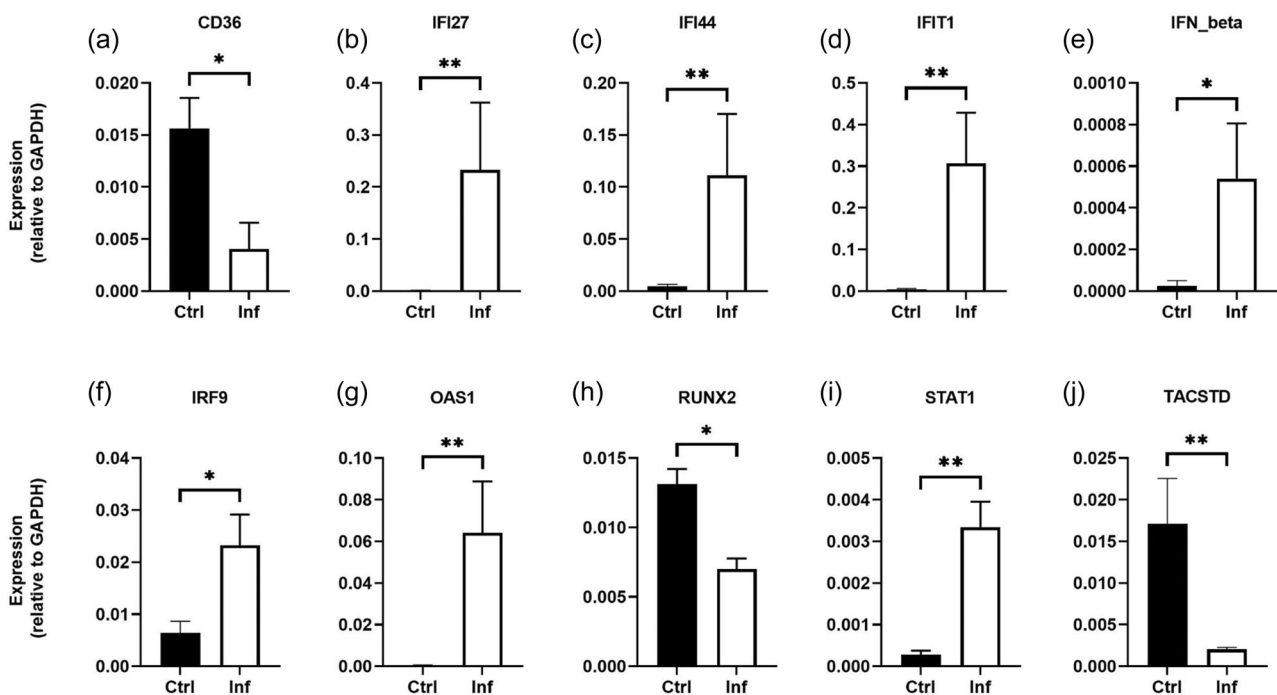

FIGURE 6 RT-qPCR validation of RNA-seq results in early stage infected MSCs. (a–j) RT-qPCR assessment of *CD36, IFI27, IFI44, IFIT1, IFN β, IRF9, OAS1, RUNX2, STAT1, and TACSTD* mRNA expression levels in early stage infected MSCs from a healthy donor (#1). Results are compared between ZIKV-infected (white bars) and mock-infected controls (black bars). Gene expression was corrected for the housekeeping gene, *GAPDH*. Error bars represent the SEM. Each group tested has *n* = 6 replicates. **p* < 0.05. MSCs, mesenchymal stromal cells; RNA-seq, RNA sequencing; SEM, standard error of the mean; ZIKV, Zika virus.
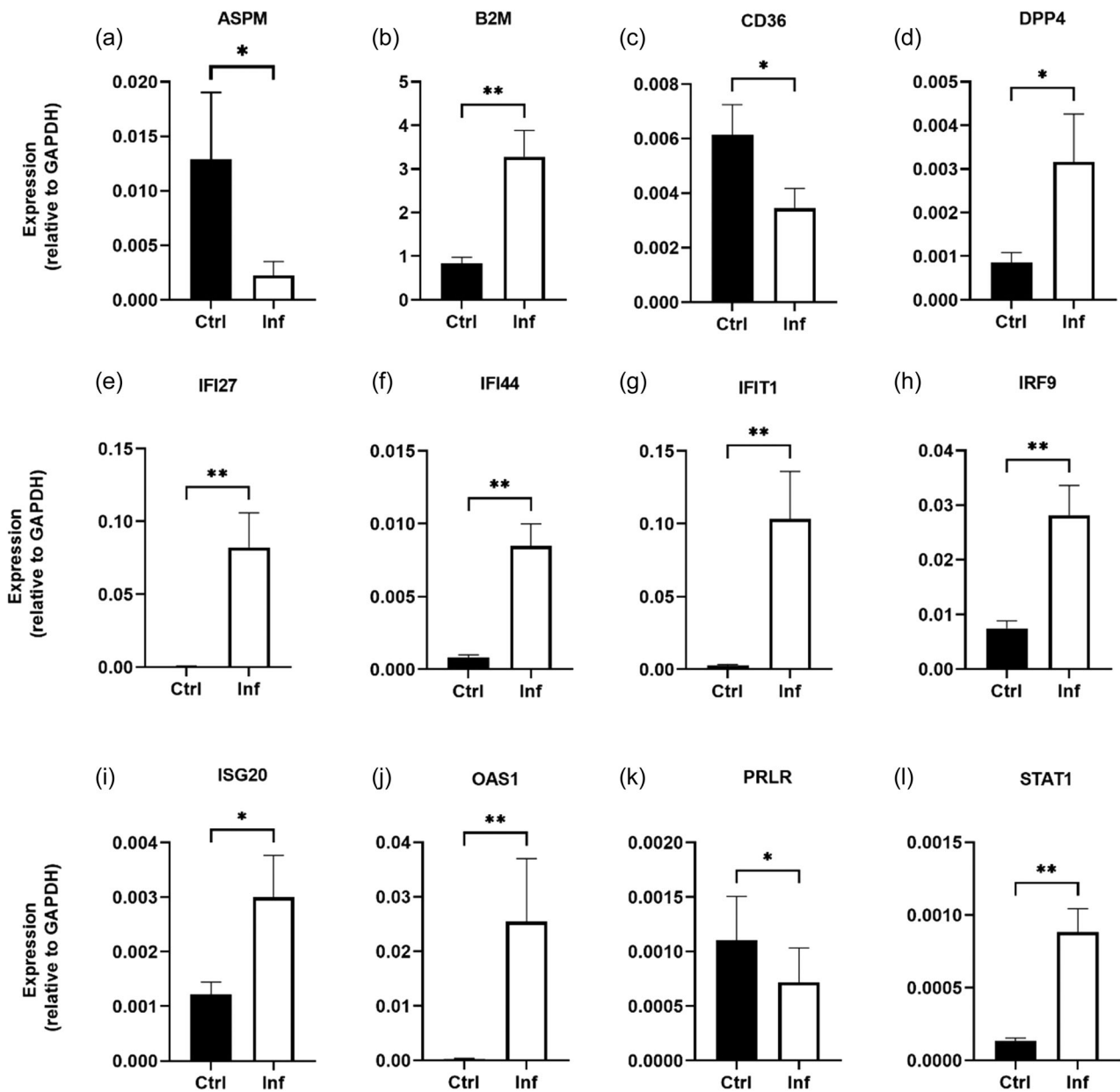
FIGURE 7 RT-qPCR validation of RNA-seq results in late stage infected MSCs. (a–l) RT-qPCR assessment of *ASPM*, *B2M*, *CD36*, *DPP4*, *IFI27*, *IFI44*, *IFIT1*, *IRF9*, *ISG20*, *OA1*, *PRLR*, and *STAT1* mRNA expression levels in late stage infected MSCs from a healthy donor (#1). Results are compared between ZIKV-infected (white bars) and mock-infected controls (black bars). Gene expression was corrected for the housekeeping gene, *GAPDH*. Error bars represent the SEM. Each group tested has $n = 6$ replicates. *$p < 0.05$. MSCs, mesenchymal stromal cells; RNA-seq, RNA sequencing; SEM, standard error of the mean; ZIKV, Zika virus.

with a developmental disorder called craniosynostosis (Katsianou et al., 2016). While ZIKV infection may increase the incidence of microcephaly by precipitating a neurological disorder (Brasil et al., 2016; Moore et al., 2017), our results suggest that ZIKV may perhaps promote premature fusion of cranial sutures by affecting CNCCs that are required for cranio-facial development (Bayless et al., 2016; Chung et al., 2009).

Host transcriptomic analysis reflects the opposing phenotypic changes following ZIKV infection in early versus later stage MSCs. Using functional enrichment analysis for ZIKV-infected early stage

MSCs, we mainly found an enrichment of genes linked to immune-related responses. It might explain the underlying factors responsible for reduced differentiation and maturation in ZIKV-infected early stage MSCs, as it was previously reported that IFN-mediated immune response could affect early stages of differentiation of MSCs and lineage-commitment toward the osteoblast phenotype (Abukawa et al., 2006; Hatzfeld et al., 2007). Early differentiating MSCs are sensitive to IFN β, which affects extracellular matrix formation and reduced mineralization, while once they are osteogenically committed, osteoblasts are insensitive to IFN exposure (Woeckel

—WILEY—

et al., 2012). These earlier findings indicate that osteogenic differentiation of MSCs may occur concomitantly with a temporally variable response to immune factors. Furthermore, genetic disorders with increased IFN activity (interferonopathies) are often linked with diverse syndromes with characteristic bone defects, including multiple skeletal dysplasia, reduced head development, osteoporosis, and so on (d'Angelo et al., 2021; Goede et al., 2006; Yu & Song, 2020). Thus, intrinsic susceptibility of MSCs to ZIKV, which is functionally linked to robust expression of the AXL receptor which mediates viral entry, triggers an IFN response that may suffice to produce cranial bone abnormalities.

Several other lines of evidence support the interpretation that perturbation of immunoregulation may alter osteoblast differentiation and bone formation. For example, endogenous type-I IFN based feedback inhibition mechanisms control bone remodeling via IFN stimulated genes and their upstream immune regulators (Deng et al., 2020). Hence, any disturbance in immune regulation can perturb bone remodeling either by affecting bone formation or bone resorption. Interferonopathies along with an enhanced proinflammatory cytokine profile are evident during viral infection as has been observed upon CHIKV infection (Chirathaworn et al., 2010). CHIKV infected patients exhibit upregulation of type 1 IFN and inflammatory cytokine profiles that are associated with arthritis, imbalanced bone remodeling, and excessive bone loss (Amdekar et al., 2017; Kelvin et al., 2011; Mori et al., 2011; Rulli et al., 2007). The mechanisms that regulate bone remodeling in physiological and pathological conditions are complex. Further studies are warranted to explore how arboviruses may alter bone homeostasis by modulating regulators of osteoimmunology that balance the differentiation and function of both osteoclasts and osteoblasts.

Osteoblast−osteoclast communication is essential to maintain bone metabolism. There is a well-regulated balance between the functions of bone-forming osteoblasts and bone-resorbing osteo-clasts (Raggatt & Partridge, 2010; Sims & Martin, 2014). Arthritogenic arboviruses, including CHIKV and RRV, are known to infect bone-forming osteoblasts (derived from MSCs) and induce the expression of proinflammatory cytokines. This subsequently triggers the activity of bone resorbing osteoclasts (hematopoietic cells) and may cause pathological bone loss (Borgherini et al., 2008; W. Chen et al., 2014). While this study addressed the potential role of osteoblasts in ZIKV pathogenesis, further studies are needed to examine the role of osteoclasts and the osteoblast−osteoclast interaction to understand how ZIKV alters bone homeostasis to induce bone pathologies.

In later stage MSCs, ZIKV infection results in changes in cell cycle progression as reflected by downregulation of DEGs that support DNA synthesis during the S phase and microtubule-mediated formation of the mitotic spindle that segregates chromosomes during mitosis. Beyond mitosis, degradation of microtubule activity is associated with increased osteogenesis in vitro and in vivo models via upregulation of bone morphogenetic protein 2 (BMP2) transcription (Brum et al., 2015; Zhao et al., 2009). Our demonstration that microtubule-binding proteins (e.g., KIF11, CENPE, KIF15, BIRCA) are downregulated, and those for BMP upregulated, suggests that arrest of cell proliferation supports the stimulation of osteogenesis following ZIKV infection of mature osteoblasts.

The cyclin-dependent kinases (CDKs) had also been investigated for their effect on osteoblast differentiation (Drissi et al., 1999; Farhat et al., 2021). In general, differentiation of osteoblasts is characterized by a well-defined sequence of maturation stages, including cell proliferation and matrix synthesis followed by extra-cellular matrix mineralization, which is regulated by temporal expression of cell cycle and phenotype-related genes. CDKs mediate phosphorylation of regulatory factors, which in turn determine the transitions between sequential phases of the cell cycle during osteoblast differentiation, while CDK inactivation by CDKN proteins suppresses cell proliferation. Our expression analysis of MSCs infected at a later stage reveals that these cells exhibit a mixed downregulation of kinase-related genes and their cognate inhibitors including CDK1, CDKN3, and CDKN2C. Changes in the expression of these genes may support cell cycle arrest and hence indirectly enhance mineralization.
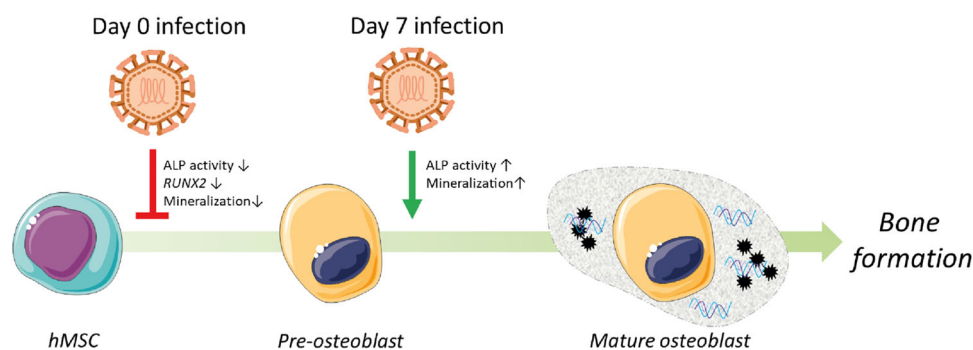

FIGURE 8 A summarized overview of ZIKV infection and phenotypic effects in early and late stage differentiating MSCs. Our previous data demonstrated that ZIKV infection of MSCs during early differentiation stages (Day 0) reduced their differentiation and maturation potential compared to mock-infected controls. In contrast to early stage infection, ZIKV infection during later stages of differentiation (Day 7 poststimulation) induced osteogenesis, in terms of ALP activity and mineralization, compared to mock-infected controls. These findings clearly demonstrate the stage-dependent phenotypic effect of ZIKV infection MSCs differentiation and osteogenesis. ALP, alkaline phosphatase; ZIKV, Zika virus.

In conclusion, we report that the biological effects of ZIKV infection on MSCs depend on the stage of osteogenic differentiation. Furthermore, we addressed the role of MSCs in determining ZIKV pathogenesis by providing the first evidence that while ZIKV-infection itself is independent of osteogenic differentiation, ZIKV has a differentiation stage-dependent effect on osteogenesis (Figure 8). Our results highlight the potential role of MSCs and osteoblast precursor cells in the pathogenesis of ZIKV and osteoarticular complications and suggest a direct role of ZIKV infected cells, rather than a bystander effect.

Future studies employing ex vivo and in vivo bone models will be required to disentangle the principal mechanism of ZIKV pathogenesis for bone-related problems in primary ZIKV infection. Apart from the risk of bone pathologies, another aspect to consider is to evaluate the role of MSCs in the pathogenesis of neurodevelopmental problems due to ZIKV infection since different MSCs populations originating from various sources have distinct functions. These investigations are critical to highlighting the pathways and molecular targets for the development of preventive and therapeutic measures.

AUTHOR CONTRIBUTIONS

Noreen Mumtaz, Bram C. J. van der Eerden, and Barry Rockx designed the experiments. Noreen Mumtaz and Marijke Koedam conducted experiments. Noreen Mumtaz, Andre J. van Wijnen, Amel Dudakovic, Asha Nair, Barry Rockx, and Bram C. J. van der Eerden analyzed and interpreted the data. Noreen Mumtaz, Andre J. van Wijnen, Barry Rockx, and Bram C. J. van der Eerden drafted the manuscript. All authors reviewed the manuscript.

ACKNOWLEDGMENTS

CONFLICT OF INTEREST

The authors declare no conflict of interest.

ORCID

Noreen Mumtaz http://orcid.org/0000-0003-2339-9766
Barry Rockx https://orcid.org/0000-0003-2463-027X
Bram C. J. van der Eerden http://orcid.org/0000-0003-4403-6497

REFERENCES

Abukawa, H., Kaban, L. B., Williams, W. B., Terada, S., Vacanti, J. P., & Troulis, M. J. (2006). Effect of interferon-alpha-2b on porcine mesenchymal stem cells. *Journal of Oral and Maxillofacial Surgery*, 64(8), 1214–1220. https://doi.org/10.1016/j.joms.2006.04.006

Alshammari, S. A., Alamri, Y. S., Rabhan, F. S., Alabdullah, A. A., Alsanie, N. A., Almarshad, F. A., & Alhaqbani, A. N. (2018). Overview of dengue and Zika virus similarity, what can we learn from the Saudi experience with dengue fever? *International Journal of Health Sciences*, 12(1), 77–82. https://www.ncbi.nlm.nih.gov/pubmed/29623022

Amdekar, S., Parashar, D., & Alagarasu, K. (2017). Chikungunya virus-induced arthritis: Role of host and viral factors in the pathogenesis. *Viral Immunology*, 30(10), 691–702. https://doi.org/10.1089/vim.2017.0052

Bayless, N. L., Greenberg, R. S., Swigut, T., Wysocka, J., & Blish, C. A. (2016). Zika virus infection induces cranial neural crest cells to produce cytokines at levels detrimental for neurogenesis. *Cell Host & Microbe*, 20(4), 423–428. https://doi.org/10.1016/j.chom.2016.09.006

Bordi, L., Avsic-Zupanc, T., Lalle, E., Vairo, F., Capobianchi, M. R., & da Costa Vasconcelos, P. F. (2017). Emerging Zika virus infection: A rapidly evolving situation. *Advances in Experimental Medicine and Biology*, 972, 61–86. https://doi.org/10.1007/5584_2016_187

Borgherini, G., Poubeau, P., Jossaume, A., Gouix, A., Cotte, L., Michault, A., Arvin-Berod, C., & Paganin, F. (2008). Persistent arthralgia associated with chikungunya virus: A study of 88 adult patients on Reunion Island. *Clinical Infectious Diseases*, 47(4), 469–475. https://doi.org/10.1086/590003

Both, T., van de Peppel, H. J., Zillikens, M. C., Koedam, M., van Leeuwen, J. P. T. M., van Hagen, P. M., van Daele, P. L. A., & van der Eerden, B. C. J. (2017). Hydroxychloroquine decreases human MSC-derived osteoblast differentiation and mineralization in vitro. *Journal of Cellular and Molecular Medicine*, 22(2), 873–882. https://doi.org/10.1111/jcmm.13373

Brasil, P., Pereira, J. P., Jr., Moreira, M. E., Ribeiro Nogueira, R. M., Damasceno, L., Wakimoto, M., Rabello, R. S., Valderramos, S. G., Halai, U. A., Salles, T. S., Zin, A. A., Horovitz, D., Daltro, P., Boechat, M., Raja Gabaglia, C., Carvalho de Sequeira, P., Pilotto, J. H., Medialdea-Carrera, R., Cotrim da Cunha, D., … Nielsen-Saines, K. (2016). Zika virus infection in pregnant women in Rio de Janeiro. *New England Journal of Medicine*, 375(24), 2321–2334. https://doi.org/10.1056/NEJMoa1602412

Bruedigam, C., Driel, M., Koedam, M., Peppel, J., van der Eerden, B. C. J., Eijken, M., & van Leeuwen, J. P. T. M. (2011). Basic techniques in human mesenchymal stem cell cultures: Differentiation into osteogenic and adipogenic lineages, genetic perturbations, and phenotypic analyses. *Current Protocols in Stem Cell Biology*, 17. https://doi.org/10.1002/9780470151808.sc01h03s17

Brum, A. M., van de Peppel, J., van der Leije, C. S., Schreuders-Koedam, M., Eijken, M., van der Eerden, B. C. J., & van Leeuwen, J. P. T. M. (2015). Connectivity Map-based discovery of parbendazole reveals targetable human osteogenic pathway. *Proceedings of the National Academy of Sciences*, 112(41), 12711–12716. https://doi.org/10.1073/pnas.1501597112

Del Campo, M., Feitosa, I. M. L., Ribeiro, E. M., Horovitz, D. D. G., Pessoa, A. L. S., França, G. V. A., García-Alix, A., Doriqui, M. J. R., Wanderley, H. Y. C., Sanseverino, M. V. T., Neri, J. I. C. F., Pina-Neto, J. M., Santos, E. S., Verçosa, I., Cernach, M. C. S. P., Medeiros, P. F. V., Kerbage, S. C., Silva, A. A., van der Linden, V., … Schuler-Faccini, L. (2017). The phenotypic spectrum of congenital Zika syndrome. *American Journal of Medical Genetics, Part A*, 173(4), 841–857. https://doi.org/10.1002/ajmg.a.38170

Chen, J., Yang, Y., Yang, Y., Zou, P., Chen, J., He, Y., Shui, S., Cui, Y., Bai, R., Liang, Y., Hu, Y., Jiang, B., Lu, L., Zhang, X., Liu, J., & Xu, J. (2018). AXL promotes Zika virus infection in astrocytes by antagonizing type I interferon signalling. *Nature Microbiology*, 3(3), 302–309. https://doi.org/10.1038/s41564-017-0092-4

Chen, W., Foo, S. S., Rulli, N. E., Taylor, A., Sheng, K. C., Herrero, L. J., Herring, B. L., Lidbury, B. A., Li, R. W., Walsh, N. C., Sims, N. A., Smith, P. N., & Mahalingam, S. (2014). Arthritogenic alphaviral

infection perturbs osteoblast function and triggers pathologic bone loss. *Proceedings of the National Academy of Sciences*, 111(16), 6040–6045. https://doi.org/10.1073/pnas.1318859111

Chen, W., Foo, S. S., Sims, N. A., Herrero, L. J., Walsh, N. C., & Mahalingam, S. (2015). Arthritogenic alphaviruses: New insights into arthritis and bone pathology. *Trends in Microbiology*, 23(1), 35–43. https://doi.org/10.1016/j.tim.2014.09.005

Chirathaworn, C., Rianthavorn, P., Wuttirattanakowit, N., & Poovorawan, Y. (2010). Serum IL-18 and IL-18BP levels in patients with Chikungunya virus infection. *Viral Immunology*, 23(1), 113–117. https://doi.org/10.1089/vim.2009.0077

Chung, I. H., Yamaza, T., Zhao, H., Choung, P. H., Shi, S., & Chai, Y. (2009). Stem cell property of postmigratory cranial neural crest cells and their utility in alveolar bone regeneration and tooth development. *Stem Cells*, 27(4), 866–877. https://doi.org/10.1002/stem.2

Colombo, T. E., Estofolete, C. F., Reis, A. F. N., da Silva, N. S., Aguiar, M. L., Cabrera, E. M. S., Dos Santos, I. N. P., Costa, F. R., Cruz, L. E. A. A., Rombola, P. L., Terzian, A. C. B., & Nogueira, M. L. (2017). Clinical, laboratory and virological data from suspected ZIKV patients in an endemic arbovirus area. *Journal of Clinical Virology*, 96, 20–25. https://doi.org/10.1016/j.jcv.2017.09.002

Cui, Y. C., Wu, Q., Teh, S. W., Peli, A., Bu, G., Qiu, Y. S., Benelli, G., & Kumar, S. S. (2018). Bone breaking infections—A focus on bacterial and mosquito-borne viral infections. *Microbial Pathogenesis*, 122, 130–136. https://doi.org/10.1016/j.micpath.2018.06.021

d'Angelo, D. M., Di Filippo, P., Breda, L., & Chiarelli, F. (2021). Type I interferonopathies in children: An overview. *Frontiers in Pediatrics*, 9, 631329. https://doi.org/10.3389/fped.2021.631329

Deng, Z., Ng, C., Inoue, K., Chen, Z., Xia, Y., Hu, X., Greenblatt, M., Pernis, A., & Zhao, B. (2020). Def6 regulates endogenous type-I interferon responses in osteoblasts and suppresses osteogenesis. *eLife*, 9, e59659. https://doi.org/10.7554/eLife.59659

Dennis, G., Jr., Sherman, B. T., Hosack, D. A., Yang, J., Gao, W., Lane, H. C., & Lempicki, R. A. (2003). DAVID: Database for annotation, visualization, and integrated discovery, *Genome Biology*, 4(5), P3. https://www.ncbi.nlm.nih.gov/pubmed/12734009

Drissi, H., Hushka, D., Aslam, F., Nguyen, Q., Buffone, E., Koff, A., van Wijnen, A., Lian, J. B., Stein, J. L., & Stein, G. S. (1999). The cell cycle regulator p27kip1 contributes to growth and differentiation of osteoblasts. *Cancer Research*, 59(15), 3705–3711. https://www.ncbi.nlm.nih.gov/pubmed/10446985

Dudakovic, A., Camilleri, E., Riester, S. M., Lewallen, E. A., Kvasha, S., Chen, X., Radel, D. J., Anderson, J. M., Nair, A. A., Evans, J. M., Krych, A. J., Smith, J., Deyle, D. R., Stein, J. L., Stein, G. S., Im, H. J., Cool, S. M., Westendorf, J. J., Kakar, S., ... van Wijnen, A. J. (2014). High-resolution molecular validation of self-renewal and spontaneous differentiation in clinical-grade adipose-tissue derived human mesenchymal stem cells. *Journal of Cellular Biochemistry*, 115(10), 1816–1828. https://doi.org/10.1002/jcb.24852

van der Eijk, A. A., van Genderen, P. J., Verdijk, R. M., Reusken, C. B., Mögling, R., van Kampen, J. J. A., Widagdo, W., Aron, G. I., GeurtsvanKessel, C. H., Pas, S. D., Raj, V. S., Haagmans, B. L., & Koopmans, M. P. G. (2016). Miscarriage associated with Zika virus infection. *New England Journal of Medicine*, 375(10), 1002–1004. https://doi.org/10.1056/NEJMc1605898

Eijken, M., Koedam, M., van Driel, M., Buurman, C. J., Pols, H. A. P., & van Leeuwen, J. P. T. M. (2006). The essential role of glucocorticoids for proper human osteoblast differentiation and matrix mineralization. *Molecular and Cellular Endocrinology*, 248(1-2), 87–93. https://doi.org/10.1016/j.mce.2005.11.034

Farhat, T., Dudakovic, A., Chung, J. H., Wijnen, A. J., & St-Arnaud, R. (2021). Inhibition of the catalytic subunit of DNA-dependent protein kinase (DNA-PKcs) stimulates osteoblastogenesis by potentiating bone morphogenetic protein 2 (BMP2) responses. *Journal of Cellular Physiology*, 236(2), 1195–1213. https://doi.org/10.1002/jcp.29927

Goede, J. S., Benz, R., Fehr, J., Schwarz, K., & Heimpel, H. (2006). Congenital dyserythropoietic anemia type I with bone abnormalities, mutations of the CDAN I gene, and significant responsiveness to alpha-interferon therapy. *Annals of Hematology*, 85(9), 591–595. https://doi.org/10.1007/s00277-006-0143-z

Granchi, D., Ochoa, G., Leonardi, E., Devescovi, V., Baglìo, S. R., Osaba, L., Baldini, N., & Ciapetti, G. (2010). Gene expression patterns related to osteogenic differentiation of bone marrow-derived mesenchymal stem cells during ex vivo expansion. *Tissue Engineering Part C: Methods*, 16(3), 511–524. https://doi.org/10.1089/ten.TEC.2009.0405

Haddow, A. D., Schuh, A. J., Yasuda, C. Y., Kasper, M. R., Heang, V., Huy, R., Guzman, H., Tesh, R. B., & Weaver, S. C. (2012). Genetic characterization of Zika virus strains: Geographic expansion of the Asian lineage. *PLoS Neglected Tropical Diseases*, 6(2), e1477. https://doi.org/10.1371/journal.pntd.0001477

Hamel, R., Dejarnac, O., Wichit, S., Ekchariyawat, P., Neyret, A., Luplertlop, N., Perera-Lecoin, M., Surasombatpattana, P., Talignani, L., Thomas, F., Cao-Lormeau, V. M., Choumet, V., Briant, L., Desprès, P., Amara, A., Yssel, H., & Missé, D. (2015). Biology of Zika virus infection in human skin cells. *Journal of Virology*, 89(17), 8880–8896. https://doi.org/10.1128/JVI.00354-15

Hatzfeld, A., Eid, P., Peiffer, I., Li, M. L., Barbet, R., Oostendorp, R. A. J., Haydont, V., Monier, M. N., Milon, L., Fortunel, N., Charbord, P., Tovey, M., & Hatzfeld, J. (2007). A sub-population of high proliferative potential-quiescent human mesenchymal stem cells is under the reversible control of interferon α/β. *Leukemia*, 21(4), 714–724. https://doi.org/10.1038/sj.leu.2404589

Huang, Y. L., Chen, S. T., Liu, R. S., Chen, Y. H., Lin, C. Y., Huang, C. H., Shu, P. Y., Liao, C. L., & Hsieh, S. L. (2016). CLEC5A is critical for dengue virus-induced osteoclast activation and bone homeostasis. *Journal of Molecular Medicine*, 94(9), 1025–1037. https://doi.org/10.1007/s00109-016-1409-0

Kalari, K. R., Nair, A. A., Bhavsar, J. D., O'Brien, D. R., Davila, J. I., Bockol, M. A., Nie, J., Tang, X., Baheti, S., Doughty, J. B., Middha, S., Sicotte, H., Thompson, A. E., Asmann, Y. W., & Kocher, J. P. A. (2014). MAP-RSeq: Mayo analysis pipeline for RNA sequencing. *BMC Bioinformatics*, 15, 224. https://doi.org/10.1186/1471-2105-15-224

Katsianou, M. A., Adamopoulos, C., Vastardis, H., & Basdra, E. K. (2016). Signaling mechanisms implicated in cranial sutures pathophysiology: Craniosynostosis. *BBA Clinical*, 6, 165–176. https://doi.org/10.1016/j.bbacli.2016.04.006

Kelvin, A. A., Banner, D., Silvi, G., Moro, M. L., Spataro, N., Gaibani, P., Cavrini, F., Pierro, A., Rossini, G., Cameron, M. J., Bermejo-Martin, J. F., Paquette, S. G., Xu, L., Danesh, A., Farooqui, A., Borghetto, I., Kelvin, D. J., Sambri, V., & Rubino, S. (2011). Inflammatory cytokine expression is associated with chikungunya virus resolution and symptom severity. *PLoS Neglected Tropical Diseases*, 5(8), e1279. https://doi.org/10.1371/journal.pntd.0001279

Lanciotti, R. S., Kosoy, O. L., Laven, J. J., Velez, J. O., Lambert, A. J., Johnson, A. J., Stanfield, S. M., & Duffy, M. R. (2008). Genetic and serologic properties of Zika virus associated with an epidemic, Yap State, Micronesia, 2007. *Emerging Infectious Diseases*, 14(8), 1232–1239. https://doi.org/10.3201/eid1408.080287

Lewallen, E. A., Trousdale, W. H., Thaler, R., Yao, J. J., Xu, W., Denbeigh, J. M., Nair, A., Kocher, J. P., Dudakovic, A., Berry, D. J., Cohen, R. C., Abdel, M. P., Lewallen, D. G., & van Wijnen, A. J. (2021). Surface roughness of titanium orthopedic implants alters the biological phenotype of human mesenchymal stromal cells. *Tissue engineering. Part A*, 27(23–24), 1503–1516. https://doi.org/10.1089/ten.TEA.2020.0369

Love, M. I., Huber, W., & Anders, S. (2014). Moderated estimation of fold change and dispersion for RNA-seq data with DESeq. 2. *Genome Biology*, 15(12), 550. https://doi.org/10.1186/s13059-014-0550-8

Marcondes, C. B., & Ximenes, M. F. F. M. (2016). Zika virus in Brazil and the danger of infestation by Aedes (Stegomyia) mosquitoes. *Revista da Sociedade Brasileira de Medicina Tropical*, 49(1), 4–10. https://doi.org/10.1590/0037-8682-0220-2015

Meertens, L., Labeau, A., Dejarnac, O., Cipriani, S., Sinigaglia, L., Bonnet-Madin, L., Le Charpentier, T., Hafirassou, M. L., Zamborlini, A., Cao-Lormeau, V. M., Coulpier, M., Missé, D., Jouvenet, N., Tabibiazar, R., Gressens, P., Schwartz, O., & Amara, A. (2017). Axl mediates ZIKA virus entry in human glial cells and modulates innate immune responses. *Cell Reports*, 18(2), 324–333. https://doi.org/10.1016/j.celrep.2016.12.045

Moore, C. A., Staples, J. E., Dobyns, W. B., Pessoa, A., Ventura, C. V., Fonseca, E. B., Ribeiro, E. M., Ventura, L. O., Neto, N. N., Arena, J. F., & Rasmussen, S. A. (2017). Characterizing the pattern of anomalies in congenital Zika syndrome for pediatric clinicians. *JAMA Pediatrics*, 171(3), 288–295. https://doi.org/10.1001/jamapediatrics.2016.3982

Mori, T., Miyamoto, T., Yoshida, H., Asakawa, M., Kawasumi, M., Kobayashi, T., Morioka, H., Chiba, K., Toyama, Y., & Yoshimura, A. (2011). IL-1 and TNF-initiated IL-6-STAT3 pathway is critical in mediating inflammatory cytokines and RANKL expression in inflammatory arthritis. *International Immunology*, 23(11), 701–712. https://doi.org/10.1093/intimm/dxr077

Mumtaz, N., Koedam, M., van den Doel, P. B., van Leeuwen, J. P. T. M., Koopmans, M. P. G., van der Eerden, B. C. J., & Rockx, B. (2018). Zika virus infection perturbs osteoblast function. *Scientific Reports*, 8(1), 16975. https://doi.org/10.1038/s41598-018-35422-3

Nowakowski, T. J., Pollen, A. A., Di Lullo, E., Sandoval-Espinosa, C., Bershteyn, M., & Kriegstein, A. R. (2016). Expression analysis highlights AXL as a candidate Zika virus entry receptor in neural stem cells. *Cell Stem Cell*, 18(5), 591–596. https://doi.org/10.1016/j.stem.2016.03.012

Perera-Lecoin, M., Meertens, L., Carnec, X., & Amara, A. (2013). Flavivirus entry receptors: An update. *Viruses*, 6(1), 69–88. https://doi.org/10.3390/v6010069

Raggatt, L. J., & Partridge, N. C. (2010). Cellular and molecular mechanisms of bone remodeling. *Journal of Biological Chemistry*, 285(33), 25103–25108. https://doi.org/10.1074/jbc.R109.041087

Rulli, N. E., Melton, J., Wilmes, A., Ewart, G., & Mahalingam, S. (2007). The molecular and cellular aspects of arthritis due to alphavirus infections. *Annals of the New York Academy of Sciences*, 1102, 96–108. https://doi.org/10.1196/annals.1408.007

Sikka, V., Chattu, V., Popli, R., Galwankar, S., Kelkar, D., Sawicki, S., Stawicki, S., & Papadimos, T. (2016). The emergence of Zika virus as a global health security threat: A review and a consensus statement of the INDUSEM joint working group (JWG. *Journal of Global Infectious Diseases*, 8(1), 3–15. https://doi.org/10.4103/0974-777X.176140

Sims, N. A., & Martin, T. J. (2014). Coupling the activities of bone formation and resorption: A multitude of signals within the basic multicellular unit. *BoneKEy Reports*, 3, 481. https://doi.org/10.1038/bonekey.2013.215

Sissoko, D., Malvy, D., Ezzedine, K., Renault, P., Moscetti, F., Ledrans, M., & Pierre, V. (2009). Post-epidemic Chikungunya disease on Reunion Island: Course of rheumatic manifestations and associated factors over a 15-month period. *PLoS Neglected Tropical Diseases*, 3(3), e389. https://doi.org/10.1371/journal.pntd.0000389

Stephens, A. S., Stephens, S. R., Hobbs, C., Hutmacher, D. W., Bacic-Welsh, D., Woodruff, M. A., & Morrison, N. A. (2011). Myocyte enhancer factor 2c, an osteoblast transcription factor identified by dimethyl sulfoxide (DMSO)-enhanced mineralization. *Journal of Biological Chemistry*, 286(34), 30071–30086. https://doi.org/10.1074/jbc.M111.253518

White, M. K., Wollebo, H. S., David Beckham, J., Tyler, K. L., & Khalili, K. (2016). Zika virus: An emergent neuropathological agent. *Annals of Neurology*, 80(4), 479–489. https://doi.org/10.1002/ana.24748

Wimalasiri-Yapa, B. M. C. R., Yapa, H. E., Huang, X., Hafner, L. M., Kenna, T. J., & Frentiu, F. D. (2020). Zika virus and arthritis/arthralgia: A systematic review and meta-analysis. *Viruses*, 12(10), 1137. https://doi.org/10.3390/v12101137

Woeckel, V. J., Eijken, M., van de Peppel, J., Chiba, H., van der Eerden, B. C. J., & van Leeuwen, J. P. T. M. (2012). IFNβ impairs extracellular matrix formation leading to inhibition of mineralization by effects in the early stage of human osteoblast differentiation. *Journal of Cellular Physiology*, 227(6), 2668–2676. https://doi.org/10.1002/jcp.23009

Yu, Z. X., & Song, H. M. (2020). Toward a better understanding of type I interferonopathies: A brief summary, update and beyond. *World Journal of Pediatrics*, 16(1), 44–51. https://doi.org/10.1007/s12519-019-00273-z

Zhao, M., Ko, S. Y., Liu, J. H., Chen, D., Zhang, J., Wang, B., Harris, S. E., Oyajobi, B. O., & Mundy, G. R. (2009). Inhibition of microtubule assembly in osteoblasts stimulates bone morphogenetic protein 2 expression and bone formation through transcription factor Gli2. *Molecular and Cellular Biology*, 29(5), 1291–1305. https://doi.org/10.1128/MCB.01566-08

SUPPORTING INFORMATION

Additional supporting information can be found online in the Supporting Information section at the end of this article.

How to cite this article: Mumtaz, N., Dudakovic, A., Nair, A., Koedam, M., van Leeuwen, J. P. T. M., Koopmans, M. P. G., Rockx, B., van Wijnen, A. J., & van der Eerden, B. C. J. (2022). Zika virus alters osteogenic lineage progression of human mesenchymal stromal cells. *Journal of Cellular Physiology*, 1–14. https://doi.org/10.1002/jcp.30933